Clusters of Hydrated Methane Sulfonic Acid $CH_3SO_3H \cdot (H_2O)_n$ ($n = 1-5$): A Theoretical Study

Liming Wang*

College of Chemistry, South China University of Technology, Guangzhou 510640, China
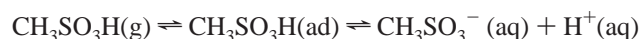
Received: November 28, 2006; In Final Form: February 12, 2007

Ab initio and density functional methods have been used to examine the structures and energetics of the hydrated clusters of methane sulfonic acid (MSA), $CH_3SO_3H \cdot (H_2O)_n$ ($n = 1-5$). For small clusters with one or two water molecules, the most stable clusters have strong cyclic hydrogen bonds between the proton of OH group in MSA and the water molecules. With three or more water molecules, the proton transfer from MSA to water becomes possible, forming ion-pair structures between $CH_3SO_3^-$ and H_3O^+ moieties. For $MSA \cdot (H_2O)_3$, the energy difference between the most stable ion pair and neutral structures are less than 1 kJ/mol, thus coexistence of neutral and ion-pair isomers are expected. For larger clusters with four and five water molecules, the ion-pair isomers are more stable (> 10 kJ/mol) than the neutral ones; thus, proton transfer takes place. The ion-pair clusters can have direct hydrogen bond between $CH_3SO_3^-$ and H_3O^+ or indirect one through water molecule. For $MSA \cdot (H_2O)_5$, the energy difference between ion pairs with direct and indirect hydrogen bonds are less than 1 kJ/mol; namely, the charge separation and acid ionization is energetically possible. The calculated IR spectra of stable isomers of $MSA \cdot (H_2O)_n$ clusters clearly demonstrate the significant red shift of OH stretching of MSA and hydrogen-bonded OH stretching of water molecules as the size of cluster increases.

I. Introduction

Methane sulfonic acid (CH_3SO_3H, MSA) and sulfuric acid are presented in the atmosphere as two main oxidation products of ocean-released dimethyl sulfide.[1,2] Because of its extremely low vapor pressure, the uptake of gas-phase H_2SO_4 by atmospheric particles plays a very important role in their formation, growth, and ultimately their size and abundance. MSA, however, is substantially more volatile, particularly at relatively low H_2O concentration found in the free troposphere.[3] Although recent investigations suggest that MSA is predominantly formed heterogeneously on large particles from the oxidation of mainly dimethyl sulfoxide (DMSO),[4−6] a small amount of MSA produced in the gas phase can be a significant growth factor for the smallest particles. The atmospheric partitioning of MSA between the gas phase and liquid aerosol phase is likely to occur due to its large Henry's law constant ($2 \times 10^7 - 10^9$ M atm^{-1})[4,7] and mass accommodation coefficient of ca. 0.1.[8,9]

It is reasonable to assume the uptake of MSA into liquid aerosol phases as a reactive process:[10]

$$CH_3SO_3H(g) \rightleftharpoons CH_3SO_3H(ad) \rightleftharpoons CH_3SO_3^- (aq) + H^+(aq)$$

where g, ad, and aq denote the MSA molecules in gaseous phase, adsorbed on the surface, and in aqueous phases. The reactive step is the deprotonation processes. The ease of MSA entering the gas/water interface depends on its ability to act as a center of nucleation with water molecules and to form clusters. Once a critical cluster size is reached, the separation of $CH_3SO_3^-$ and hydrated proton occurs, and MSA merges with the bulk at the interface. Experiments have been carried out to measure the uptake coefficient of near unity for MSA to salted or acid

solution;[8,9] however, it is difficult to obtain information experimentally at molecular level, even though the techniques such as surface vibrational sum frequency spectroscopy (VSFG) can provide some structural information.[11] A simplified strategy is to study the structure and spectroscopy of the $MSA \cdot (H_2O)_n$ clusters so as the solvation and ionization processes.

The ability of MSA to nucleate with water molecules is determined by the strength of hydrogen bond formed between MSA and water molecules. The initial attempts are the studies of structure and vibrational spectra of $MSA \cdot H_2O$ monohydrate isolated in argon matrix[12] and the molecular structure of MSA at surface of neat and aqueous solution using surface VSFG technique.[11] It was found that the MSA molecule on the surface possesses a preferred orientation with the methyl group pointed away from the surface, and the adsorption of MSA induces significant structure change of the surrounding surface water clusters as indicated by the red shift of water molecule vibrational stretching modes, which arises most likely from the formation of hydrogen bonds between MSA and water molecules and the formation of protonated water clusters.

Previous studies on the hydration of acids[13−19] show that the proton transfer depends strongly on the size of the clusters, and proton transfer normally occurs at a critical size. Since MSA is a strong acid, we would expect that proton transfer takes place at sizes similar to the hydrate clusters of hydrochloride acid,[13] sulfuric acid,[14,18] halosulfonic acids,[15] CF_3SO_3H,[16] etc. In present work, the structure, energetics, and vibrational spectra of $MSA \cdot (H_2O)_n$ clusters are investigated using theoretical calculations.

II. Computational Details

The density functional theory (DFT) and molecular orbital theory calculations are carried out using Gaussian 03 suite of programs.[20] The DFT method using Becke's 3-parameter hybrid

* Tel: +86 20 87112900. Fax: +86 20 87112906. E-mail: wanglm@scut.edu.cn.

TABLE 1: Zero-Point Energies (ZPE, in Hartree), Electronic Energies (*E*, in Hartree), and Stabilization Energies (Δ*H* and Δ*G*, in kJ/mol) of CH$_3$SO$_3$H·(H$_2$O)$_n$ Relative to CH$_3$SO$_3$H + *n*H$_2$O with ZPE Corrections at Theoretical Levels of B3LYP without and with BSSE Correction (B3LYP-CP) and G3XMP2

				B3LYP	B3LYP-CP	G3XMP2		
	ZPE	B3LYP	G3XMP2	ΔH_0	ΔH_0	ΔH_0	ΔH_{298}	ΔG_{298}
I-1	0.08575	−740.96592	−740.07253	−38.3	−34.3	−41.8	−45.2	−6.0
I-2	0.08556	−740.96494	−740.07146	−36.2	−32.2	−39.5	−42.6	−3.7
I-3	0.08429	−740.95590	−740.06307	−15.8		−22.0	−21.4	10.7
I-4	0.08430	−740.95603	−740.06318	−16.1		−22.4	−21.6	10.6
II-1	0.11029	−817.44484	−816.45477	−77.8	−69.4	−78.3	−85.0	−7.0
II-2	0.11029	−817.44475	−816.45485	−77.6	−69.1	−78.6	−85.1	−7.2
II-3	0.10997	−817.44328	−816.45323	−74.6	−66.3	−75.1	−81.2	−4.9
II-4	0.11038	−817.44518	−816.45519	−78.5	−69.9	−79.2	−85.8	−7.3
II-5	0.10902	−817.43409	−816.44693	−52.9	−47.1	−61.1	−64.8	5.6
II-6	0.10908	−817.43421	−816.44701	−53.1	−47.1	−61.1	−64.9	6.1
II-7	0.10916	−817.43490	−816.44784	−54.7	−48.8	−63.1	−66.9	3.9
II-8	0.10910	−817.43501	−816.44792	−55.1	−49.2	−63.5	−67.2	2.9
II-9	0.10941	−817.43814	−816.44856	−62.6	−55.2	−64.3	−68.3	−1.0
II-10	0.10926	−817.43671	−816.44709	−59.2	−52.0	−60.9	−64.5	2.5
III-1	0.13532	−893.92293	−892.83780	−113.9	−101.3	−115.7	−128.6	0.0
III-2	0.13547	−893.92133	−892.83819	−109.3	−96.3	−116.3	−126.5	−5.0
III-3	0.13482	−893.92271	−892.83607	−114.6		−112.4	−121.8	−6.6
III-4	0.13376	−893.91432	−892.83060	−95.3	−84.8	−100.8	−107.9	1.8
III-5	0.13481	−893.91435	−892.83085	−92.7	−80.5	−98.7	−107.6	9.1
III-6	0.13482	−893.91449	−892.82982	−93.0	−81.6	−96.0	−104.4	9.3
III-7	0.13407	−893.91179	−892.82819	−87.9	−76.8	−93.7	−101.1	11.7
III-8	0.13396	−893.90974	−892.82656	−82.8	−72.5	−89.7	−96.2	12.9
III-9	0.13512	−893.91243	−892.82771	−86.8	−76.3	−89.7	−97.9	13.8
III-10	0.13502	−893.91230	−892.82751	−86.7	−76.5	−89.4	−97.5	13.7
IV-1	0.16017	−970.40308	−969.22062	−155.8	−149.9	−152.9	−168.5	−3.7
IV-2	0.16083	−970.40124	−969.22129	−149.2	−131.9	−152.9	−169.4	0.9
IV-3	0.16063	−970.40273	−969.21979	−153.7	−135.9	−149.5	−166.2	1.9
IV-4	0.16093	−970.39790	−969.21772	−140.2	−122.7	−143.3	−157.1	6.2
IV-5	0.15944	−970.39706	−−969.21534	−141.9	−124.0	−141	−152.9	1.3
IV-6	0.15938	−970.39327	−969.21503	−132.1	−115.6	−140.3	−152.4	6.8
IV-7	0.15760	−970.39063	−969.21242	−129.8	−114.1	−138.1	−148.7	4.5
IV-8	0.16026	−970.39351	−969.21196	−130.4	−114.0	−129.9	−142.5	12.9
V-1	0.18480	−1046.88128	−1045.60165	−193.2	−172.4	−186.0	−204.1	−3.6
V-2	0.18535	−1046.87986	−1045.60191	−188.0	−165.5	−185.3	−204.5	1.1
V-3	0.18553	−1046.86964	−1045.59682	−161.2	−140.2	−171.9	−190.1	16.9
V-4	0.18420	−1046.86348	−1045.59074	−148.0	−128.4	−158.9	−175.3	25.6

functional together with Lee−Yang−Parr correlation functional (B3LYP[21,22]) has been employed for geometry optimization and vibrational frequency evaluations with a triple-ζ basis set 6-311+G(2df,p) as implemented in Gaussian 03. The zero-point energy (ZPE) corrections are obtained from the computed DFT vibrational frequencies scaled by 0.9854.[23] Geometries have also been confirmed at MP2 level using the same basis set. Single point electronic energies are calculated at theoretical levels of B3LYP and MP2 using 6-311+G(2df,p) basis set, and Gaussian-3X with reduced MP2 expansion (G3XMP2).[23−25] For comparison, energies are also calculated at full G3X level for MSA· H$_2$O and MSA·(H$_2$O)$_2$. The DFT stabilization energies of MSA· (H$_2$O)$_n$ to MSA + *n*H$_2$O are corrected for basis set superposition error (BSSE) using the full counterpoise method (B3LYP-CP).[26,27]

III. Results and Discussions

The geometries of CH$_3$SO$_3$H and CH$_3$SO$_3$H·(H$_2$O)$_n$ (*n* = 1−5) have been optimized at B3LYP and MP2 levels using 6-311+G(2df,p) basis set (Figures 1-5). Since MSA·(H$_2$O)$_n$ clusters can normally be viewed as the complexes between MSA and water clusters or between CH$_3$SO$_3$$^-$ and protonated water clusters, the geometries of neutral and protonated water clusters are also optimized. The initial geometries of water clusters and their protonated forms are obtained from previous studies.[28−32] For sulfur-containing species, previous studies have shown that the DFT-B3LYP method with small double-ζ basis sets tends to overestimate the bond lengths such as the S=O bond in DMSO, while MP2 predictions with triple-ζ basis sets are in

better agreement with the experimental measurements.[33,34] Present predictions indicate that 6-311+G(2df,p) basis set is yet not large enough. For "normal" chemical bonds, the DFT bond lengths are usually shorter than the MP2 ones which should be closer to the real values. Subsequently, the electronic energies of MP2 structures at G3X and/or G3XMP2 levels are always lower than those of B3LYP ones, even though the differences are always less than 2 kJ/mol, i.e., the differences for CH$_3$-SO$_3$H and CH$_3$SO$_3$$^-$ are 1.7 and 1.4 kJ/mol, respectively. We will base our discussions on B3LYP geometries.

The electronic energies at B3LYP and G3XMP2 levels are listed in Table 1. Previous studies on the thermochemical properties for sulfur-containing molecules and reactions found that the theoretical results depend strongly on the level of correlation and the size of the basis sets even if the isodesmic reactions are used.[34−36] MP2 always predicts higher stabilization energies than B3LYP and G3XMP2 for MSA·(H$_2$O)$_n$ clusters. Similar trend has also been observed in previous study.[37] The B3LYP stabilization energies agree well with the G3XMP2 ones; however, discrepancies are significant after BSSE corrections. The correlation level of the G3XMP2 method is approximately QCISD(T)/G3eXlarge, therefore being considered as the most reliable in present study. Discussions will be based on the G3XMP2 stabilization energies of MSA·(H$_2$O)$_n$ relative to MSA + *n*H$_2$O. For comparison, G3X results for mono- and dihydrates will also be presented.

A. Methane Sulfonic Acid and Its Monohydrates. Figure 1shows the structures of methane sulfonic acid and its mono-hydrate optimized using the MP2 and B3LYP methods with
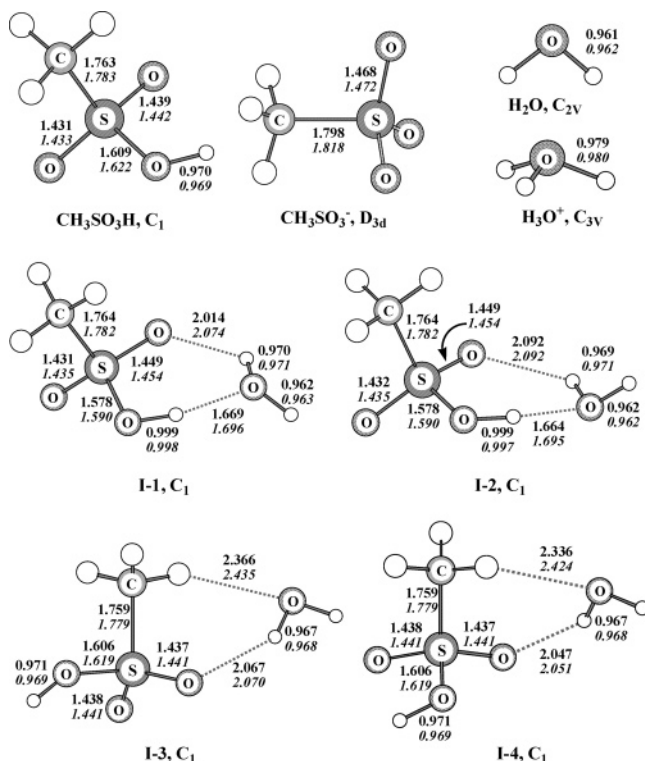
Figure 1. Optimized structures of MSA and MSA·H₂O complex determined with MP2 and B3LYP (*in italics*) methods using 6-311+G-(2df,p) basis sets. The bond lengths are in Å.

6-311+G(2df,p) basis set. Various possible hydrogen-bonded complex between MSA and H₂O have been examined and four structures have been identified (Figure 1). The first two structures agree with the ones identified by Givan et al. at B3LYP/aug-cc-pVTZ (AVTZ) level.[12] The most stable structure (I-1) has a cyclic form with a strong hydrogen bond (1.696 Å, B3LYP) between the oxygen atom of water and the proton of MSA and a weak hydrogen bond (2.074 Å) between the hydrogen atom of water and one oxygen atom of S=O bond in MSA. Structure I-2 differs from I-1 by only a flip-flop of the dangling OH bond of the water molecule relative to the cyclic plane with a transition barrier of about 1.1 kJ/mol at B3LYP/ AVTZ level.[12] Structures I-3 and I-4 have only one weak hydrogen bond (2.070 and 2.051 Å, respectively) which is formed between the O-atom of S=O bond of MSA and one H-atom in water.

Of the four complexes identified, I-1 is the most stable one. For I-1, the strong hydrogen bond causes the elongation of the O—H bond of MSA and the shortening of the S—OH bond from the isolated MSA, and leads to the stabilization of the system by 41.8 kJ/mol at 0 K and 45.2 kJ/mol at 298 K at G3XMP2 level (44.3 and 47.6 kJ/mol at G3X level). The S=O bond is also lengthened slightly by the weak hydrogen bond. The Gibbs free energy change upon formation of I-1 is −6.0 kJ/mol (G3XMP2) at 298 K; i.e., the I-1 formation can take place to certain extend at ambient condition. Compared to I-1, complex I-2 is slightly less stable by 2.7 kJ/mol. Once formed, its conversion to I-1 will be extremely fast because of the small transition barrier. Complexes I-3 and I-4 are *ca.* 23 kJ/mol above I-1, leading to their negligible population at room temperatures. The relative energy of −37.7 kJ/mol at 298 K predicted by B3LYP-CP for I-1 agrees with the previous prediction of −35.9 kJ/mol at B3LYP/AVTZ level also with BSSE correction.[12] On the other hand, the relative energy of −45.2 kJ/mol at 298 K for CH₃SO₃H·H₂O—I-1 at G3XMP2 level is comparable to the

fitted value of 44.3 kJ/mol for H₂SO₄·H₂O from the experimental pressure data.[38]

Similar cyclic structures with hydrogen bonds have also been found in H₂SO₄·H₂O, CF₃SO₃H·H₂O, and XSO₃H·H₂O (X = F, Cl, Br) complexes with similar bond length changes. For the most stable complexes, the stabilization energy is 42.7 kJ/mol for H₂SO₄·H₂O at B3LYP/D95++(d,p) level,[14] 57.7 kJ/mol for CF₃SO₃H·H₂O[16] and 44.0−48.1 kJ/mol for halosulfonic acids at B3LYP/6-311++G(d,p) level,[15] compared to 34.3 kJ/mol for MSA·H₂O-1 here at B3LYP/6-311+G(2df,p).

B. CH₃SO₃H·(H₂O)₂ Cluster. Figure 2 depicts the optimized structures for the dihydrated complex CH₃SO₃H·(H₂O)₂. In structures II-(1−4), the water dimer is bonded to MSA through one strong (1.539−1.550 Å) and one weak (1.863−1.882 Å) hydrogen bonds, forming a cyclic structure. Compared to the monohydrates I-1 and I-2, these structures have further shortening of the S—OH bond lengths, elongation of SO—H bonds (1.021−1.025 Å), and shortening of the SOH—OH₂ hydrogen bond. The hydrogen bond lengths within the (H₂O)₂ dimer (1.721−1.746 Å) are also much shorter than that in isolated water dimer (1.940 Å). Structures II-(1−4) differ only on the orientations of the dangling O—H bonds in water molecules, and interconversion between them should be extremely fast as that between I-1 and I-2. Structures II-(1−4) represent the most stable CH₃SO₃H·(H₂O)₂ clusters with the largest G3XMP2 stabilization energy of 79.2 kJ/mol (84.9 by G3X) relative MSA + 2H₂O and 67.0 kJ/mol relative to MSA + (H₂O)₂ for II-4. Similar structures have the lowest energies for H₂SO₄·(H₂O)₂, CF₃SO₃H·(H₂O)₂, and XSO₃H·(H₂O)₂ clusters as well. The B3LYP-CP stabilization energy of 69.9 kJ/mol for II-4 with 6-311+G(2df,p) basis set is smaller than those of 87.5 kJ/mol for H₂SO₄·(H₂O)₂ with DP95++(d,p) basis set,[14] of 114.9 kJ/ mol for CF₃SO₃H·(H₂O)₂, and 91.6−94.6 kJ/mol for XSO₃H· (H₂O)₂ (X = F, Cl, Br) with 6-311++G(d,p) basis set.[15,16]

The structures II-(5−8) are combinations of the two types of hydrogen bonds observed in MSA·H₂O. The lengths of the hydrogen bonds are not significantly different from those in monohydrates, and the stabilization energies (61−64 kJ/mol, G3XMP2) are also approximately the summation of those in monohydrates (41.8 and 22.4 kJ/mol for I-1 and I-4). Namely, the binding of two water molecules can be considered as independent of each other.

Structures II-9 and II-10 can be viewed as the binding between MSA and one molecule of the water dimer. This hydrogen bonding is stronger that those in monohydrates I-1 and I-2. Compared to I-1/2, the S—OH and SO—H bond lengths in II-9/10 are further slightly shortened, and the hydrogen bond SOH—OH₂ is significantly shortened by *ca.* 0.1 Å, and the hydrogen bond within (H₂O)₂ shortened by *ca.* 0.11 Å from the free (H₂O)₂ dimer. The binding energies between MSA and (H₂O)₂ are 52.1 and 48.7 kJ/mol for II-9 and II-10 (G3XMP2), respectively, being stronger than those between MSA and H₂O in monohydrates (41.8 and 39.5 kJ/mol for I-1 and I-2). The differences between structures II-(1−4) and II-9/10 are *ca.* 16 kJ/mol, being close to the difference of *ca.* 17 kJ/mol between similar structures in H₂SO₄·(H₂O)₂.[14]

C. CH₃SO₃H·(H₂O)₃ Cluster. From the cases of H₂SO₄· (H₂O)₃, HCl·(H₂O)₃, and XSO₃H·(H₂O)₃ clusters,[13−15] one might expect the proton transfer from MSA to water molecule and the coexistence of neutral and ion-pair clusters for MSA· (H₂O)₃. Figure 3 depicts the optimized structures of various isomers of MSA·(H₂O)₃. There are three most stable isomers III-(1−3). Structure III-1 is a proton-transferred ion-pair complex with symmetry of C_S point group. The structure is
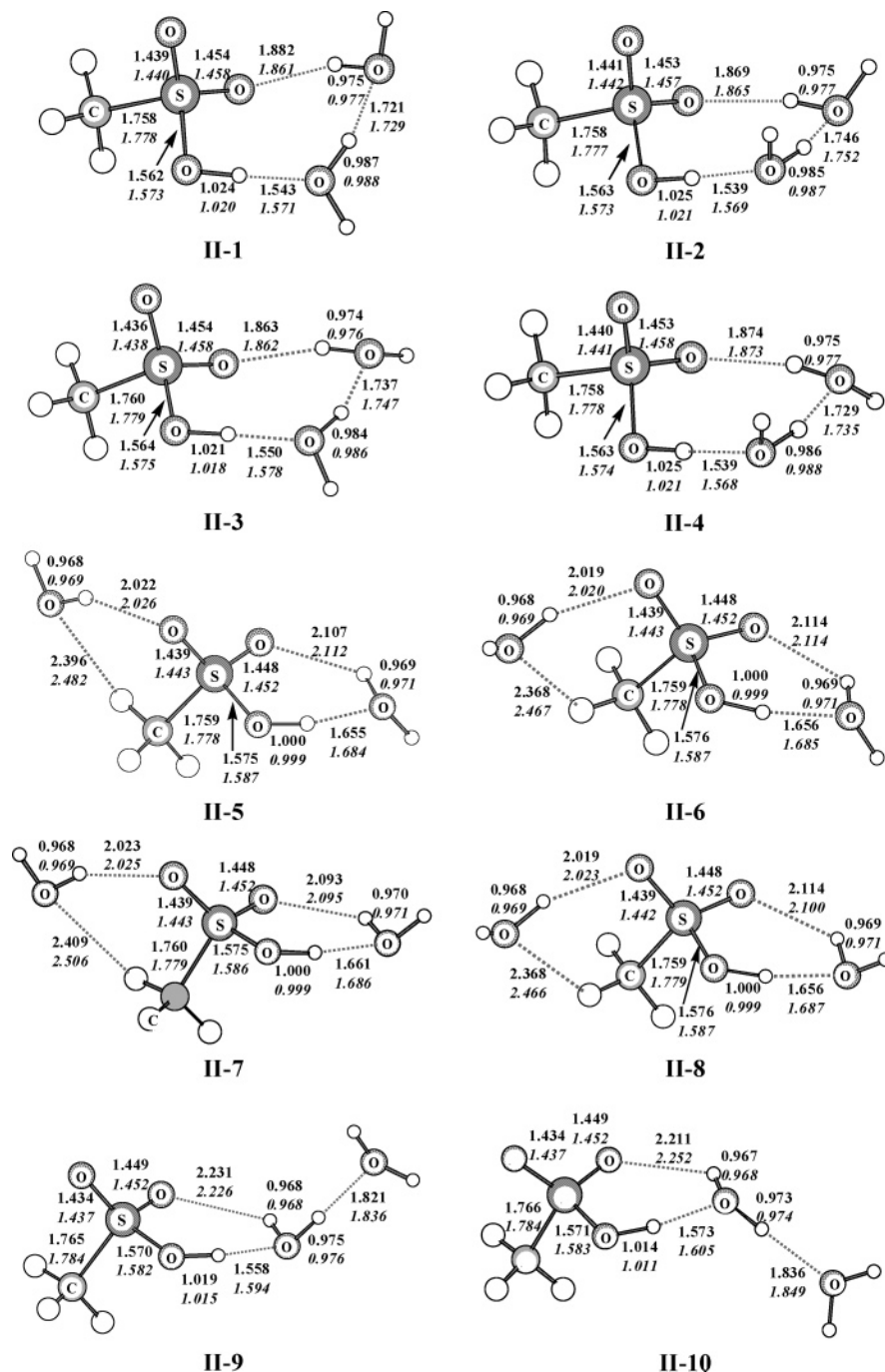
Figure 2. Optimized structures of stable isomers of MSA·(H₂O)₂ calculated at B3LYP and MP2 levels with 6-311+G(2df,p) basis set.

characterized by two strong cyclic hydrogen bonds between CH₃SO₃⁻ and H₃O⁺ moieties, and positive charge (+0.74, natural charge[39]) is located on H₃O⁺ and negative charge (−0.81) on CH₃SO₃⁻ moiety. All three hydrogen atoms of the H₃O⁺ ion form strong hydrogen bonds (one 1.423 and two 1.568 Å) which stabilize this structure, along with two other hydrogen bonds (1.747 Å). The conformation of H₇O₃⁺ moiety in complex III-1 is close to that of free H₇O₃⁺, though the hydrogen bond between H₂O and H₃O⁺ is somewhat weaker. Structures III-2 and III-3 have no proton transfer between MSA and water. Structure III-2 has six hydrogen bonds, the most among all MSA·(H₂O)₃ isomers located here, therefore being the most stable. Cluster III-3 has only four hydrogen bonds, forming a large cyclic structure. However, all these hydrogen bonds possess almost linear structures which maximize the bond strength and minimize the strain energy.

The relative stability of III-1−3 depends on the level of theory employed. At B3LYP level, the neutral structure III-3 is the most stable, and the ion pair III-1 is less than 1 kJ/mol above it. At MP2 level, III-1 becomes the most stable structure with the neutral III-2 being higher by *ca.* 4−5 kJ/mol. At G3XMP2 level, III-2 becomes the most stable isomer, while the energy difference between the III-1 and III-2 is less than 1 kJ/mol. Nevertheless, the small energy difference implies the coexistence of ion-pair form III-1 and neutral form3 III-2/3 for MSA·(H₂O)₃ clusters. Note that the BSSE correction for B3LYP calculations of III-1 is relative to CH₃SO₃⁻ + H₃O⁺ + 2H₂O, and similarly for larger ion-pair clusters. The difference to MSA + nH₂O is the BSSE correction for the reaction energy of CH₃SO₃H + H₂O → CH₃SO₃⁻ + H₃O⁺, which should be negligible.

Figure 3 also shows the optimized structures of other less stable conformers for MSA·(H₂O)₃ clusters. The relative stable
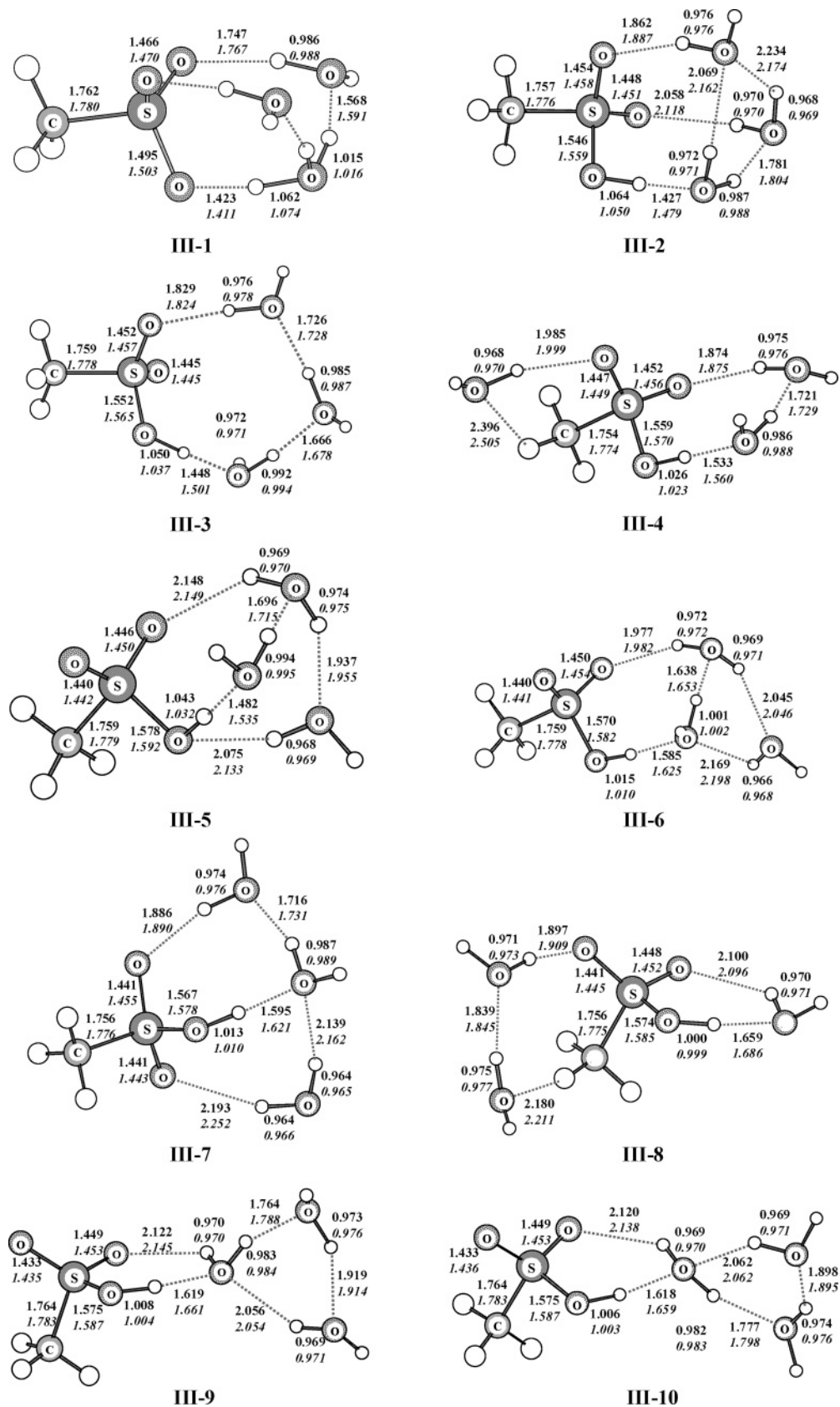
Figure 3. Optimized structures of stable isomers of MSA·(H₂O)₃ calculated at B3LYP and MP2 levels with 6-311+G(2df,p) basis set.

structures III-(4−7) have cyclic forms between MSA and a water dimer (H₂O)₂ with the third water bonded to S=O bond in MSA (III-4), to OH group in MSA and one molecule in (H₂O)₂ (III-5), to (H₂O)₂ (III-6), and to S=O bond in MSA and one molecule in (H₂O)₂ (III-7), respectively. The energy difference

between III-4 and III-7 is ca. 7 kJ/mol. Structure III-4 can be viewed as almost independent combination of the weak hydrogen bonds in MSA·H₂O of I-3/4 and the strong cyclic ones in MSA·(H₂O)₂ of II-(1−4), and the stabilization energy of 101 kJ/mol relative to MSA + 3H₂O (G3XMP2) is approximately
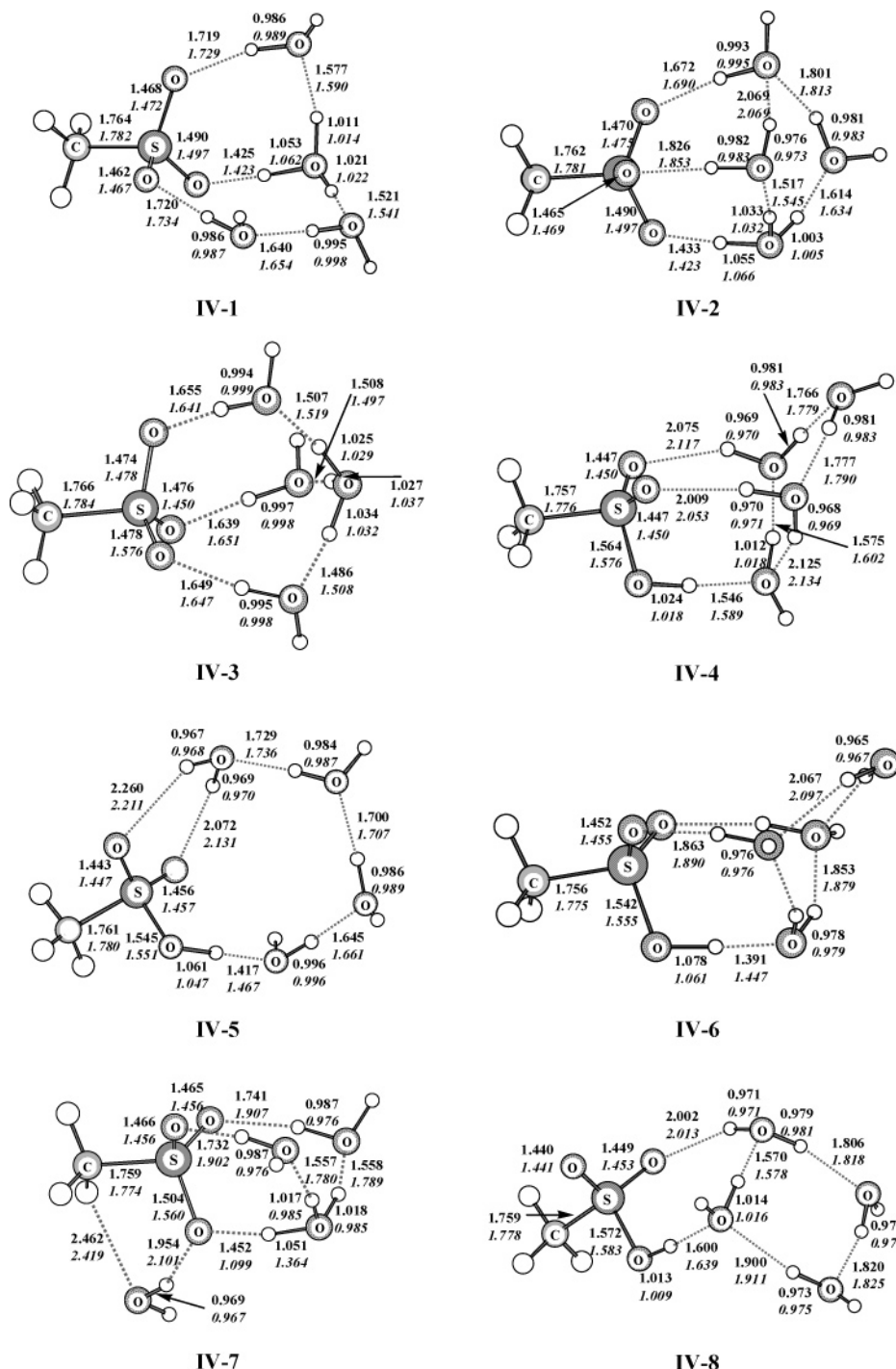
Figure 4. Optimized structures of stable isomers of MSA·(H₂O)₄ calculated at B3LYP and MP2 levels with 6-311+G(2df,p) basis set.

the summation of those in I-4 (21 kJ/mol) and II-4 (79 kJ/mol). Similar structures are expected to have different orientations of dangling O−H bond in H₂O molecules as in II-(1−4) and the H₂O bonding to S=O bond as in I-3/4; however, these structures are also expected to be nearly degenerate in energy.

The least stable structures III-(8−10) have one strong cyclic hydrogen bond between MSA and one water molecule. In structure III-8, one water dimmer is hydrogen bonded to MSA through one weak hydrogen bond with O-atom of S=O bond and one with H-atom of CH₃ group in MSA. In structures III-9/10, the water dimer is hydrogen bonded to the strongly bonded water molecule, and they can be viewed as the bonding between MSA and one water molecule in (H₂O)₃. No further effort is undertaken to exhaust all possible conformations of dangling

OH bonds. The bond lengths of S−OH and SOH−OH₂ in III-9/10 are between those in I-1/2 and II-(1−4) (see Figures 1−3); subsequently, the G3XMP2 bonding strength of *ca.* 47 kJ/mol between MSA + (H₂O)₃ in III-9/10 is slightly higher than those between MSA + H₂O (41.7 and 39.3 kJ/mol for I-1 and I-2), and lower than those between MSA + (H₂O)₂ (67 kJ/mol for II-4).

D. CH₃SO₃H·(H₂O)₄ Cluster. Figure 4 shows the optimized structures of MSA·(H₂O)₄ clusters. Similar to those in H₂SO₄· (H₂O)₄ clusters, the ionic structures of MSA·(H₂O)₄ clusters can be classified into two groups. In IV-1/2, the H₃O⁺ moiety interacts directly with CH₃SO₃⁻, while in IV-3, indirectly via one water molecule. In these structures, position charges on H₃O⁺ moiety are *ca.* 0.71−0.75, and strong hydrogen bonds
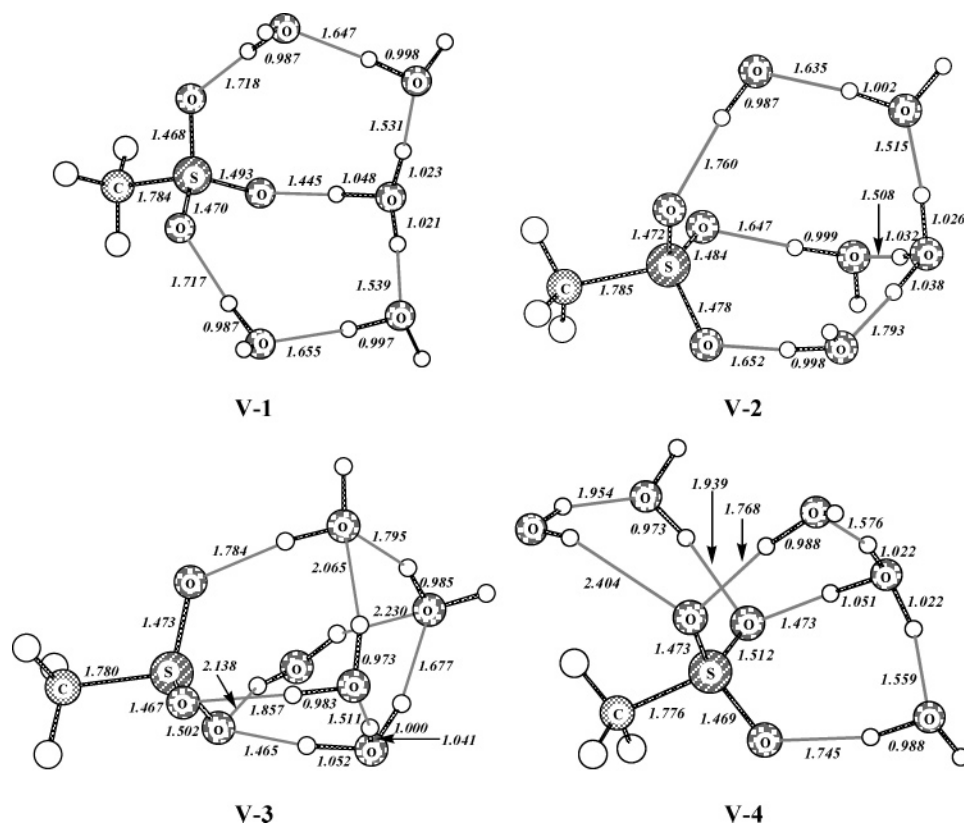
Figure 5. Optimized structures of stable isomers of MSA·(H$_2$O)$_5$ calculated at B3LYP level with 6-311+G(2df,p) basis set.

are formed between H$_3$O$^+$ and water molecules and/or CH$_3$SO$_3^-$ to stabilize the system. Structure IV-3 has pseudo C_s symmetry. Structures with different orientation of dangling OH bonds of water are located as well for IV-1 and IV-3 (not shown in Figure 4), however, to have approximately equal stability. The energy differences between three ion-pair structures are less than 3 kJ/ mol, being similar to H$_2$SO$_4$·(H$_2$O)$_4$ ionic clusters.[14] Structures IV-2 and IV-3 can be viewed as the complex between CH$_3$SO$_3^-$ and H$_9$O$_4^+$ bonded by hydrogen bonds and Coulomb interaction. The H$_9$O$_4^+$ moiety in IV-2 corresponds to the cyclic free H$_9$O$_4^+$ and in IV-3 the pyramidal one. Even though the cyclic H$_9$O$_4^+$ is ∼10 kJ/mol less stable than the pyramidal one, the energy difference between structures IV-2 and IV-3 are <2 kJ/mol since the short distance between position and negative charge centers in IV-2 leads to stronger Coulomb interaction.

For MSA·(H$_2$O)$_4$ clusters, the proton-transferred ion-pair structures are at lower energies than non-transferred neutrals at all levels of theory employed in present study. The energy difference between the most stable structures of ion pair IV-1 and neutral IV-4 is ca. 10 kJ/mol at G3XMP2 level, i.e., the ion-pair structures are much favored over the neutral ones. This is similar to CF$_3$SO$_3$H and halosulfonic acid systems,[15,16] while it is significantly different from H$_2$SO$_4$·(H$_2$O)$_4$ clusters, for which the energy difference between the most stable ion pair and neutral is less than 4 kJ/mol, and it is hard to conclude which isomer is the most stable.[14] The equal stability of ionic and neutral H$_2$SO$_4$·(H$_2$O)$_4$ is due to the capability of two OH groups in H$_2$SO$_4$ in forming strong neutral hydrogen bonds.

As illustrated in Figure 4, the most stable neutral isomer IV-4 has hydrogen bond between MSA and three water molecules of most stable (H$_2$O)$_4$ tetramer,[29] while isomer IV-8 has a hydrogen bond between MSA and two water molecules of (H$_2$O)$_4$ and is less stable than IV-4 by ca. 14 kJ/mol. Structures IV-4, 6, and 7 can be viewed as III-1 (MSA + water trimer) with an additional water molecule added; however, the proton

is not transferred from MSA to water here. It is noticed that DFT and MP2 methods behave differently on isomer IV-7, for which DFT predicts an ionic structure while MP2 a neutral one, even though they have almost the same relative stability at G3XMP2 level. The stabilization energy of 138.9 kJ/mol for IV-7 relative to MSA + 4H$_2$O is approximately the sum of that in III-1 and I-4 (115.4 and 22.1 kJ/mol, respectively), indicating that the interactions of MSA + (H$_2$O)$_3$ and MSA + H$_2$O are almost independent of each other.

E. CH$_3$SO$_3$H·(H$_2$O)$_5$ Cluster. Although there must be many isomers of CH$_3$SO$_3$H·(H$_2$O)$_5$ clusters due to the various combination of hydrogen-bonding sites, the most stable structures are expected to be ionic as for MSA·(H$_2$O)$_4$. The possible conformations have been built by simply adding one additional water molecule to the stable MSA·(H$_2$O)$_4$ isomers and pre-optimize their geometries at B3LYP/6-31G(d) level. The final four geometries optimized at B3LYP/6-311+G(2df,p) level is shown in Figure 5, all being ion pairs. In structures V-1/3/4, the CH$_3$SO$_3^-$ and H$_3$O$^+$ moieties are bonded through direct hydrogen bonds, and in structure V-2 indirectly via water molecules. In structures V-1 and V-2, all water molecules are bonded through strong hydrogen bonds (bond lengths less than 1.8 Å), thus being the most stable, while structure V-3 can be viewed as MSA·(H$_2$O)$_4$ IV-1 with an additional weakly bonded water, and V-4 as MSA·(H$_2$O)$_3$ III-1 with a weakly bonded water dimer. The energy difference between structure V-1 and V-2 is less than 1 kJ/mol, but structures V-3 and V-4 are ca. 14 kJ/mol or more higher. The equal stability of direct and indirect bonding between CH$_3$SO$_3^-$ and H$_3$O$^+$ moieties implies that separation of positive and negative charge becomes energetically possible at such cluster size, while for H$_2$SO$_4$·(H$_2$O)$_5$, the indirect one is less stable by ca. 4 kJ/mol.[14] The proton nontransferred CH$_3$SO$_3$H·(H$_2$O)$_5$ clusters are expected to have relatively weak hydrogen bonds between water molecules; and will be energetically less favored.

TABLE 2: Calculated Vibrational Frequencies of CH$_3$SO$_3^-$ and CH$_3$SO$_3$H at B3LYP and MP2 Level with 6-311+G(2df,p) Basis Set, and Their Comparison to Experimental Values

| | CH$_3$SO$_3^-$ | | CH$_3$SO$_3$H | | | | | | |
	B3LYP freq	MP2 freq	B3LYP freq	DFT I_{IR}	MP2 freq	MP2 I_{IR}	expt (in Ar)	expt (gas)	description
1	212	227	183	56.4	194	56.8			CH$_3$ and OH torsion
2	313	321	207	17.4	224	16.0			CH$_3$ torsion
3	313	321	310	12.1	318	10.6			CSO bend
4	508	517	322	14.9	333	18.6			CH$_3$ wag
5	508	517	429	14.3	440	17.3	454.4	473	O-S-OH deform
6	524	546	484	19.4	495	21.6	496.5	502	SO$_2$ anti-sym deform
7	724	758	509	39.8	526	42.7	526.9	528	SO$_3$ sym deform
8	948	961	718	39.3	760	43.9	746.5	748	S-OH and C-S stretch pseudo sym
9	948	961	803	218.8	839	214.0	832.5	828	S-OH and C-S stretch pseudo anti-sym
10	1015	1049	981	2.8	989	3.6	967.0	980	CH$_3$ rock
11	1206	1245	991	29.5	999	34.1	975.3	980	CH$_3$ rock
12	1206	1245	1122	27.0	1121	41.4	1118.3	1122	SOH bend
13	1308	1325	1186	216.2	1218	196.0	1193.6	1202	SO$_2$ sym stretch
14	1460	1478	1357	12.9	1372	19.3	1332.8	1336	CH$_3$ sym deform
15	1460	1478	1389	285.1	1430	276.4	1393.4	1403	SO$_2$ anti-sym stretch
16	3038	3074	1457	5.3	1474	5.5	1422.1	1418	CH$_3$ anti-sym deform
17	3128	3187	1459	0.5	1478	4.1	1434.0	1418	CH$_3$ anti-sym deform
18	3128	3187	3066	0.1	3097	0.2	3047.0		CH$_3$ sym stretch
19			3160	0.2	3213	0.9	3188.5		CH$_3$ anti-sym stretch
20			3170	0.1	3222	0.4	3204.5		CH$_3$ anti-sym stretch
21			3777	132.3	3782	149.5	3579.4	3609	O-H stretch

F. Free Energy Changes and Fraction of Hydrated Clusters. From Table 1, the G3XMP2 stabilization energies of MSA·(H$_2$O)$_n$ relative to MSA + nH$_2$O are 41.8 (I-1), 79.2 (II-4), 115.7 (III-1), 152.9 (IV-1, ionic), and 186.0 (V-1) kJ/mol for $n = 1-5$, respectively, for the most stable isomers. It is ca. 36 kJ/mol for each successive hydration. The values are 34.3, 69.9, ∼102.0, 149.9, and 172.4 kJ/mol at B3LYP/6-311+G-(2df,p) level with BSSE corrections. The interactions are weaker than those of 44, 87, 130, 177, and 213 kJ/mol for H$_2$SO$_3$H·(H$_2$O)$_n$,[14] those of 57.7, 114.9, 162.9, 239.0, and 282.6 kJ/mol for CF$_3$SO$_3$H·(H$_2$O)$_n$,[16] and those for XSO$_3$H·(H$_2$O)$_n$ (X = F, Cl, and Br).[15] This is consistent with the fact that H$_2$SO$_4$, CF$_3$-SO$_3$H, and halosulfonic acids are stronger acids than CH$_3$SO$_3$H, and CF$_3$SO$_3^-$ and XSO$_3^-$ are more stable than CH$_3$SO$_3^-$.

The estimated Gibbs free energy changes for MSA + nH$_2$O → MSA·(H$_2$O)$_n$ using the DFT geometries and vibrational frequencies (treated as harmonic oscillators) are −6.0, −7.3, −6.6, −3.7, and −3.6 kJ.mol at 298 K for I-1, II-4, III-3, IV-1, and V-1, respectively, at G3XMP2 level. Since the frequencies for intermolecular vibrational modes are greatly underestimated when they are treated as harmonic oscillators,[40] entropies of the clusters are overestimated. Thereafter, the ΔG values should be smaller. The upper limits of the equilibrium constants K_n are 11.3, 19.0, 14.3, 4.4, and 4.3 atm^{-1} at 25 °C. From {P[MSA ·(H$_2$O)$_n$]}/{P[MSA]} = K_nP[H$_2$O]^n and the low vapor pressure of H$_2$O (∼0.03 atm), only the formations of mono- and dihydrates are significant at room temperature, with fractions of 0.34 and 0.018. At lower temperatures, the equilibrium constants are larger while the water vapor pressures are lower, e.g., K_1(0 °C) = 53 and K_1(−10 °C) = 113, K_2(0 °C) = 483 and K_2(−10 °C) = 2000 atm^{-1}, while P(0 °C) = 6.03 × 10^{-3} and P(−10 °C) = 2.83 × 10^{-3} atm.[41] The monohydrate is still the dominant form with fractions of 0.32 and 0.32 and the dihydrates of 0.0160 and 0.0176 at −10 and 0 °C. The ability of MSA to form hydrated clusters is weaker than that of H$_2$-SO$_4$, where K_1 = 656 and K_2 = 86.0 atm^{-1} at 25 °C;[38] therefore being less efficient in forming new condensation nuclei.

G. Vibrational Analysis. The infrared spectra of MSA, (MSA)$_2$, and MSA·H$_2$O have been studied experimentally and theoretically.[12,33] Theoretical prediction showed that IR spectrum of gaseous MSA is indeed from (MSA)$_2$, and spectra of MSA·

H$_2$O in argon matrix are also accompanied by additional bands from MSA and (MSA)$_2$. Even though it is necessary to account for the vibrational unharmonicity in order to predict precisely the frequencies for species with hydrogen bonds, especially for low-frequency intermolecular modes,[29,40] the tasks demand large computational resources. It is usually adequate to apply one or more scale factors.[29] Tables 2 and 3 list the comparisons between theory and experiment for MSA and MSA·H$_2$O. The values for intermolecular modes are largely underestimated comparing to vibrational self-consistent calculations;[40] therefore, the corresponding values in Table 3 are for reference only. For MSA and MSA·H$_2$O, the agreement between the unscaled MP2 frequencies and experimental measurements for low frequencies (<ca. 1300 cm^{-1}) are within 20 cm^{-1} with a few exceptions for monohydrate (bold in Table 3), while the B3LYP method tends to underestimate the low frequencies (<ca. 900 cm^{-1}). Both MP2 and B3LYP methods predict higher values for high frequencies. A difference between DFT and MP2 is noticed on the CH$_3$ antisymmetric stretch modes in MSA. At DFT level, the CH$_3$ modes are isolated from O-H stretch mode of MSA, thus the transition moment and IR intensity is negligible, while at MP2 level, the CH$_3$ modes are mixed with O-H stretch modes, thus a noticeably strong IR transition is obtained. However, this can hardly be resolved experimentally since the difference in frequency is less than 10 cm^{-1}. Since the DFT calculations are available to large clusters and the features of the IR spectra will be dominated by the strong absorptions at high-frequency range, the discussions below will be based on DFT frequencies. The B3LYP vibrational frequencies and infrared transition intensities of other clusters can be obtained from the author upon request.

One significant observation upon hydration is the red shift of the O-H stretching mode in MSA due to the formation of strong hydrogen bonds, similar to typical hydrogen-bonded systems.[13,14,42] The B3LYP frequencies are 3777, 3194, 2786, and 2323 cm^{-1} for MSA, I-1, II-4, and III-2, respectively, where proton is not transferred. The corresponding O-H bond lengths are 0.970, 0.999, 1.025, and 1.064 Å. The stretching vibrational modes of OH bonds in H$_2$O and H$_3$O$^+$ moieties are red-shifted as well when forming hydrogen bonds. As noticed above, the OH bonds are significantly stretched when forming hydrogen

TABLE 3: Calculated Vibrational Frequencies of Two Isomers of CH₃SO₃H·H₂O at B3LYP and MP2 Level with 6-311+G(2df,p) Basis Set, and their Comparison to Experimental Values

	$CH_3SO_3H \cdot H_2O$ I-1				I-2			
	B3LYP	I_{IR} (DFT)	MP2	I_{IR} (MP2)	B3LYP	MP2	expt	description
1	35	8.9	36	8.8	39	32		intermolecular
2	153	20.8	160	19.9	149	156		intermolecular
3	200	2.5	213	3.9	197	209		CH₃ torsion
4	217	18.1	229	1.3	216	223		intermolecular
5	259	105.0	251	130.5	239	232		intermolecular
6	296	7.9	304	4.5	296	302		C−S−OH bend
7	325	0.9	332	1.2	322	315		C−S=O bend
8	350	93.4	352	101.5	328	335		intermolecular
9	455	25.8	462	34.3	462	470		OSO bend
10	499	17.8	508	19.4	496	502		OSO bend
11	515	39.4	532	46.3	511	522	534.2	SO₃ stretch
12	576	201.3	558	160.5	551	540		intermolecular
13	733	24.0	775	21.8	733	776	761.3	C−S stretch
14	**816**	**119.2**	**842**	**118.5**	**788**	**812**	**877.2**	**OH torsion MSA**
15	855	194.1	891	189.6	854	891	884.1	S−OH stretch
16	982	3.3	991	4.2	981	990		CH₃ rock
17	**993**	**42.1**	**1002**	**53.0**	**993**	**1002**	**979.7**	**CH3 rock**
18	1153	164.6	1193	165.9	1152	1191	1173.1	SO₂ sym stretch
19	**1317**	**181.6**	**1341**	**129.4**	**1317**	**1334**	**1304.0**	**SO2 anti-sym stretch**
20	1358	20.2	1372	27.6	1356	1372		CH₃ sym def
21	**1408**	**218.0**	**1431**	**270.6**	**1400**	**1423**	**1334.0**	**SOH bend**
22	1458	4.0	1474	4.2	1458	1474		CH₃ anti-sym def
23	1460	3.2	1479	7.6	1459	1477		CH₃ anti-sym def
24	1619	75.1	1612	77.0	1617	1611	1600.0	HOH bend in water
25	3065	0.3	3095	0.3	3066	3097		CH₃ sym stretch
26	3161	2.1	3212	179.7	3161	3212		CH₃ anti-sym stretch
27	3167	0.1	3218	1.5	3168	3219		CH₃ anti-sym stretch
28	3194	1217.4	3208	1065.3	3210	3219	2930.0	OH stretch in MSA
29	3704	153.4	3744	119.1	3712	3753	3539.2	HB-bonded OH stretch in water
30	3875	118.9	3917	148.4	3883	3927	3687.2	dangling OH stretch in water

bond. A correlation between the red shift of vibrational frequencies and the bond lengths for all OH bonds forming hydrogen bonds are illustrated in Figure 6a. The red shift is approximately proportional to the lengthening of O−H bond caused by the hydrogen bond, and the largest shifts are due to the hydrogen bonds with H₃O⁺ moieties and with OH group of MSA moiety. On the other hand, the IR transition intensity of these O−H stretching modes is also greatly enhanced (Figure 6b). For the dangling OH bonds in water molecules, the unscaled DFT frequencies fall in the range of 3850−3950 cm⁻¹ and the IR intensities around 100 km/mol. Note that the correlation here applies only to the OH bonds forming strong hydrogen bonds with hydrogen bond length less than ca. 1.9 Å, so that the O−H stretching mode is almost a local mode. For weakly bonded H₂O molecule, the O−H stretching can be treated as pseudo symmetric and antisymmetric modes.
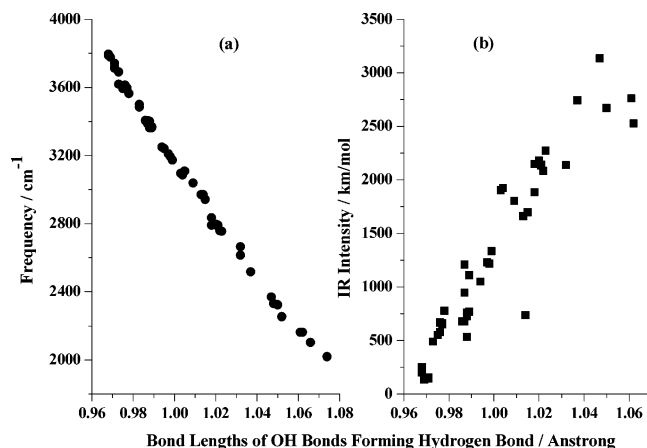

Figure 6. The correlations for O−H bonds forming hydrogen bonds in MSA·(H₂O)ₙ (n = 0−5): (a) vibrational frequencies vs OH bond lengths; (b) Infrared transition intensities vs O−H bond lengths.

The features of the IR spectra of hydrated clusters are dominated by the OH-stretching modes forming strong hydrogen bonds. The absorptions below 2000 cm⁻¹ are weak, compared to the OH stretching modes, and the ionic clusters have larger absorptions than the neutral ones. For ion-pair isomer III-1, three strong peaks can be assigned to the three O−H stretching modes from H₃O⁺. With the increase of the number of water molecules, peaks between 2000 and 3000 cm⁻¹ are still prominent, while strong transitions from other strong hydrogen-bonded O−H stretching appears. These strong transitions are red-shifted from the pure water clusters, and they agree qualitatively with the VSFS observation of MSA on aqueous surfaces.[11]

IV. Conclusions

The hydration process of methane sulfonic acid has been studied using ab initio and DFT calculations. Because of the multiple sites of MSA and capability of water in hydrogen bond formation, the CH₃SO₃H·(H₂O)ₙ clusters have various isomers. Strong hydrogen bonds are formed between OH group of MSA and water molecules. With the size of the clusters increased to three water molecules, the ionic isomers with proton transferred from MSA to water appears, forming CH₃SO₃⁻ and H₃O⁺ moieties in the clusters. For CH₃SO₃H·(H₂O)₃ clusters, the energy of the ionic isomer is not significantly different from the neutral ones; thus a coexistence of ionic and neutral isomers is expected. For CH₃SO₃H·(H₂O)₄ clusters and larger, the ionic structures have lower energy than the neutral ones, and the ionic clusters will dominate the population. The stabilization energies of the most stable MSA·(H₂O)ₙ isomers relative to MSA + nH₂O are 41.8 (I-1), 79.1 (II-4), 115.6 (III-1), 152.8 (IV-1, ionic), and 186.0 kJ/mol at G3XMP2 level for n = 1−5, respectively. The stabilization energies are close to those in H₂SO₄·(H₂O)ₙ clusters, while smaller than those for CF₃SO₃H·(H₂O)ₙ and XSO₃H·(H₂O)ₙ.[14−16] The formation of strong

hydrogen bonds also causes strong red shift of O−H vibrational stretching mode and greatly enhances the IR transition of these modes when the OH bond participates hydrogen bond formation. A good correlation is found between the lengthening of the bonds and the magnitude of the red shifts, while it is only an approximation with the enhancement of the IR transition. The red shift is in qualitative agreement with the observed spectra of MSA on air-aqueous solution interfaces using VSFS technique.

References and Notes

(1) Ravishankara, A. R.; Rudich, Y.; Talukdar, R.; Barone, S. B. *Philos. Trans. Royal Soc. London, Ser. B* **1997**, *352*, 171.

(2) Ayers, G. P.; Cainey, J. M.; Gillett, R. W.; Ivey, J. P. *Philos. Trans. Royal Soc. London, Ser. B* **1997**, *352*, 203.

(3) Eisele, F. L.; McMurry, P. H. *Philos. Trans. Royal Soc. London, Ser. B* **1997**, *352*, 191.

(4) Campolongo, F.; Saltelli, A.; Jensen, N. R.; Wilson, J.; Hjorth, J. *J. Atmos. Chem.* **1999**, *32*, 327.

(5) von Glasow, R.; Crutzen, P. J. *Atmos. Chem. Phys.* **2004**, *4*, 589.

(6) Barnes, I.; Hjorth, J.; Mihalopoulos, N. *Chem. Rev.* **2006**, *106*, 940.

(7) Clegg, S. L.; Brimblecombe, P. *Environ. Technol. Lett.* **1985**, *6*, 269.

(8) Hanson, D. R. *J. Phys. Chem. A* **2005**, *109*, 6919.

(9) Schweitzer, F.; Magi, L.; Mirabel, P.; George, C. *J. Phys. Chem. A* **1998**, *102*, 593.

(10) Davidovits, P. *Chem. Rev.* **2006**, *106*, 1323.

(11) Allen, H. C.; Raymond, E. A.; Richmond, G. L. *J. Phys. Chem. A* **2001**, *105*, 1649.

(12) Givan, A.; Loewenschuss, A.; Nielsen, C. J. *J. Mol. Struct.* **2005**, *748*, 77.

(13) Re, S.; Osamura, Y.; Suzuki, Y.; Schaefer, H. F. I. *J. Chem. Phys.* **1998**, *109*, 973.

(14) Re, S.; Osamura, Y.; Morokuma, K. *J. Phys. Chem. A* **1999**, *103*, 3535.

(15) Li, S.; Tao, F.-M.; Gu, R. *Chem. Phys. Lett* **2006**, *426*, 1.

(16) Chaiwongwattana, S.; Sagarik, K.; Tao, F.-M. Molecular Structure and Proton Transfer in Small Clusters of Trifluoromethanesulfonic Acid with Water Molecules. 40th Western Regional Meeting of the American Chemical Society; Anaheim, CA, Jan 22−25, 2006; American Chemical Society: Washington, DC, 2006.

(17) Bianco, R.; Wang, S.; Hynes, J. T. *J. Phys. Chem. B* **2005**, *109*, 21313.

(18) Smith, A.; Vincent, M. A.; Hiller, I. H. *J. Phys. Chem. A* **1999**, *103*, 1132.

(19) Arstila, H.; Laasonen, K.; Laaksonen, A. *J. Chem. Phys.* **1998**, *108*, 1031.

(20) Frisch, M. J.; Trucks, G. W.; Schlegel, H. B.; Scuseria, G. E.; Robb, M. A.; Cheeseman, J. R.; Montgomery, J., J. A.; Vreven, T.; Kudin, K. N.; Burant, J. C.; Millam, J. M.; Iyengar, S. S.; Tomasi, J.; Barone, V.; Mennucci, B.; Cossi, M.; Scalmani, G.; Rega, N.; Petersson, G. A.; Nakatsuji, H.; Hada, M.; Ehara, M.; Toyota, K.; Fukuda, R.; Hasegawa, J.; Ishida, M.; Nakajima, T.; Honda, Y.; Kitao, O.; Nakai, H.; Klene, M.; Li, X.; Knox, J. E.; Hratchian, H. P.; Cross, J. B.; Bakken, V.; Adamo, C.; Jaramillo, J.; Gomperts, R.; Stratmann, R. E.; Yazyev, O.; Austin, A. J.; Cammi, R.; Pomelli, C.; Ochterski, J. W.; Ayala, P. Y.; Morokuma, K.; Voth, G. A.; Salvador, P.; Dannenberg, J. J.; Zakrzewski, V. G.; Dapprich, S.; Daniels, A. D.; Strain, M. C.; Farkas, O.; Malick, D. K.; Rabuck, A. D.; Raghavachari, K.; Foresman, J. B.; Ortiz, J. V.; Cui, Q.; Baboul, A. G.; Clifford, S.; Cioslowski, J.; Stefanov, B. B.; Liu, G.; Liashenko, A.; Piskorz, P.; Komaromi, I.; Martin, R. L.; Fox, D. J.; Keith, T.; Al-Laham, M. A.; Peng, C. Y.; Nanayakkara, A.; Challacombe, M.; Gill, P. M. W.; Johnson, B.; Chen, W.; Wong, M. W.; Gonzalez, C.; Pople, J. A. *Gaussian 03*, Revision B.05; Gaussian, Inc.: Wallingford, CT, 2004.

(21) Becke, A. D. *J. Chem. Phys.* **1993**, *98*, 5648.

(22) Lee, C.; Yang, W.; Parr, R. G. *Phys. Rev. B* **1988**, *37*, 785.

(23) Curtiss, L. A.; Redfern, P. C.; Raghavachari, K.; Pople, J. A. *J. Chem. Phys.* **2001**, *114*, 108.

(24) Curtiss, L. A.; Raghavachari, K.; Redfern, P. C.; Rassolov, V.; Pople, J. A. *J. Chem. Phys.* **1998**, *109*, 7764.

(25) Curtiss, L. A.; Redfern, P. C.; Raghavachari, K.; Rassolov, V.; Pople, J. A. *J. Chem. Phys.* **1999**, *110*, 4703.

(26) Boys, S. F.; Bernardi, F. *Mol. Phys.* **1970**, *19*, 553.

(27) Simon, S.; Duran, M.; Dannenberg, J. J. *J. Chem. Phys.* **1996**, *105*, 11024.

(28) Parthasarathi, R.; Subramanian, V. Characterization of hydrogen bonding: From van der Waals interactions to covalency. In *Hydrogen Bonding - New Insights*; Grabowski, S. J., Ed.; Springer: Dordrecht, The Netherlands, 2006; p 1.

(29) Day, M. B.; Kirschner, K. N.; Shields, G. C. *J. Phys. Chem. A* **2005**, *109*, 6773.

(30) Guissani, Y.; Guillot, B.; Bratos, S. *J. Chem. Phys.* **1988**, *88*, 5850.

(31) Xantheas, S. S.; Dunning, T. H. *J. Chem. Phys.* **1994**, *98*, 8037.

(32) Fowler, J. E.; Schaefer, H. F. I. *J. Am. Chem. Soc.* **1995**, *117*, 446.

(33) Durig, J. R.; Zhou, L.; Schwartz, T.; Gounev, T. *J. Raman Spectrosc.* **2000**, *31*, 193.

(34) Wang, L. M.; Zhang, J. S. *J. Mol. Struc. (Theochem)* **2002**, *581*, 129.

(35) Gomes, J. R. B.; Riveiro, da Silva, M. A. V. *J. Phys. Chem. A* **2004**, *108*, 11684.

(36) Resende, S. M.; Ornellas, F. R. *Chem. Phys. Lett.* **2003**, *367*, 489.

(37) Rablen, P. R.; Lackman, J. W.; Jorgensen, W. L. *J. Phys. Chem. A* **1998**, *102*, 3782.

(38) Noppel, M. *J. Geophys. Res. [Atmos]* **2000**, *105*, 19779.

(39) Gelndening, E. D.; Reed, A. E.; Carpenter, J. E.; Weinhold, F. NBO Version 3.1.

(40) Miller, Y.; Chaban, G. M.; Gerber, R. B. *J. Phys. Chem. A* **2005**, *109*, 6565.

(41) In *CRC Handbook of Chemistry and Physics*, 84th ed.; Lide, D. R., Ed.; CRC Press LLC: Boca Raton, FL, 2003.

(42) In *Hydrogen Bonding - New Insights*; Grabowski, S. J., Ed.; Springer: Dordrecht, The Netherlands, 2006.